Current Biology 24, 2307–2313, October 6, 2014 ©2014 Elsevier Ltd All rights reserved http://dx.doi.org/10.1016/j.cub.2014.08.022

Report

Kinesin-12 Kif15 Targets Kinetochore Fibers through an Intrinsic Two-Step Mechanism

Emma G. Sturgill,[1] Dibyendu Kumar Das,[2] Yoshimasa Takizawa,[1] Yongdae Shin,[3] Scott E. Collier,[1] Melanie D. Ohi,[1] Wonmuk Hwang,[4,5] Matthew J. Lang,[2] and Ryoma Ohi[1,*]

[1]Department of Cell and Developmental Biology, Vanderbilt University Medical Center, Nashville, TN 37232, USA
[2]Department of Chemical and Biomolecular Engineering, Vanderbilt University, Nashville, TN 37235, USA
[3]Department of Mechanical Engineering, Massachusetts Institute of Technology, Cambridge, MA 02139, USA
[4]Department of Biomedical Engineering, Texas A&M, College Station, TX 77843, USA
[5]School of Computational Sciences, Korea Institute for Advanced Study, Seoul 130-722, Korea

Summary

Proteins that recognize and act on specific subsets of microtubules (MTs) enable the varied functions of the MT cytoskeleton. We recently discovered that Kif15 localizes exclusively to kinetochore fibers (K-fibers) [1, 2] or bundles of kinetochore-MTs within the mitotic spindle. It is currently speculated that the MT-associated protein TPX2 loads Kif15 onto spindle MTs [3–5], but this model has not been rigorously tested. Here, we show that Kif15 accumulates on MT bundles as a consequence of two inherent biochemical properties. First, Kif15 is self-repressed by its C terminus. Second, Kif15 harbors a nonmotor MT-binding site, enabling dimeric Kif15 to crosslink and slide MTs. Two-MT binding activates Kif15, resulting in its accumulation on and motility within MT bundles but not on individual MTs. We propose that Kif15 targets K-fibers via an intrinsic two-step mechanism involving molecular unfolding and two-MT binding. This work challenges the current model of Kif15 regulation and provides the first account of a kinesin that specifically recognizes a higher-order MT array.

Introduction

Kinesins fulfill a variety of cellular functions involving the microtubule (MT) cytoskeleton. At the onset of mitosis, kinesins alter the organization and dynamics of MTs to catalyze spindle assembly [6]. The design principles of each mitotic kinesin appear to be optimally tuned for a specific task [7]. For example, the Kinesin-5 Eg5 tetramerizes to slide antiparallel MTs apart [8] and thereby establish spindle bipolarity [9]. The Kinesin-12 Kif15 has been likened to Eg5 for its ability to power spindle assembly [3, 4] as has been shown in Eg5-inhibitor-resistant cells [1, 10]. Its biochemical properties and molecular function(s) during cell division, however, remain largely unknown.

Unlike Eg5, Kif15 preferentially localizes to kinetochore fibers (K-fibers; [1, 2]), or bundles of spindle MTs that attach end-on to kinetochores. K-fiber-specific localization is unusual, demonstrated by a small cohort of molecular motors and MT-associated proteins (MAPs) such as TPX2, Astrin, Kif18A, and HURP [11–15]. The mechanisms by which these factors target K-fibers are generally not well understood but are of obvious importance given the role of K-fibers during mitosis. Intrinsic biophysical properties could drive K-fiber-specific accumulation. This is true for Kif18A, as it enriches on K-fibers as a consequence of its ultraprocessive motility [16, 17]. Alternatively, intermediary factors could facilitate MT recruitment. In the case of Kif15, TPX2 has been suggested to function in this capacity [3–5].

Here, we show that Kif15 is predisposed to bind MT bundles and elucidate the biochemical properties that cause it to do so. First, Kif15 activity is suppressed by its C-terminal Coil-2. Consistent with previous reports of self-repression, the hydrodynamic properties of Kif15 vary as a function of ionic strength. This suggests that intramolecular electrostatic interactions mediate Kif15 switching between active "open" and inactive "closed" conformations. Second, Kif15 harbors a nonmotor MT-binding site in its Coil-1, which it uses in conjunction with its motor heads to crosslink and slide MTs. Single Kif15 molecules accumulate on and walk within MT bundles, suggesting that two-MT binding locks Kif15 in a derepressed state. We propose that Kif15 autonomously targets K-fibers by activating selectively on MT bundles.

Results

Kif15-MT Binding Is Prevented by Its C Terminus during Interphase

Kif15 fails to colocalize with MTs during interphase despite being cytosolic (Figure S1A available online [4]). To test whether Kif15 can transiently bind interphase MTs, we infused cells with AMPPNP. Kinesins lock onto MTs upon treatment with this nonhydrolyzable ATP analog, making brief MT-binding events detectable [18, 19]. Endogenous Kif15 fails to colocalize with interphase MTs in AMPPNP-infused cells (Figure S1A). Exogenously expressed full-length Kif15 (GFP-Kif15-FL, Figure 1A) also remains diffuse in AMPPNP-infused interphase cells (Figure 1B). In contrast to full-length Kif15, C-terminally truncated Kif15 (GFP-Kif15-N700, Figure 1A) decorates interphase MTs in a manner enhanced by AMPPNP (Figure 1B). These data indicate that Kif15-MT binding is prevented by its C terminus during interphase.

Kif15 Motility Is Self-Repressed by Coil-2 In Vitro

Some kinesins inhibit their own activity by conformational folding [20]. Motivated by our cellular data, we tested whether Coil-2 (amino acids 961–1374, Figure 1A) inhibits Kif15 activity in vitro by capitalizing on Coil-2-targeting antibodies (αC2; [1]). We reasoned that αC2 would derepress Kif15 by preventing Coil-2 interaction(s) with the motor heads. In conventional MT gliding assays, recombinant GFP-Kif15-FL (Figures 1A and S1B) moves MTs at 0.059 ± 0.029 μm s^{-1} (average ±SD, n = 1,374, Figures S1C and S1D; Movie S1). But when anchored to flow cells by αC2, GFP-Kif15-FL glides MTs at 0.123 ± 0.071 μm s^{-1} (n = 1,804, Figures S1C and S1D; Movie S1).

*Correspondence: ryoma.ohi@vanderbilt.edu

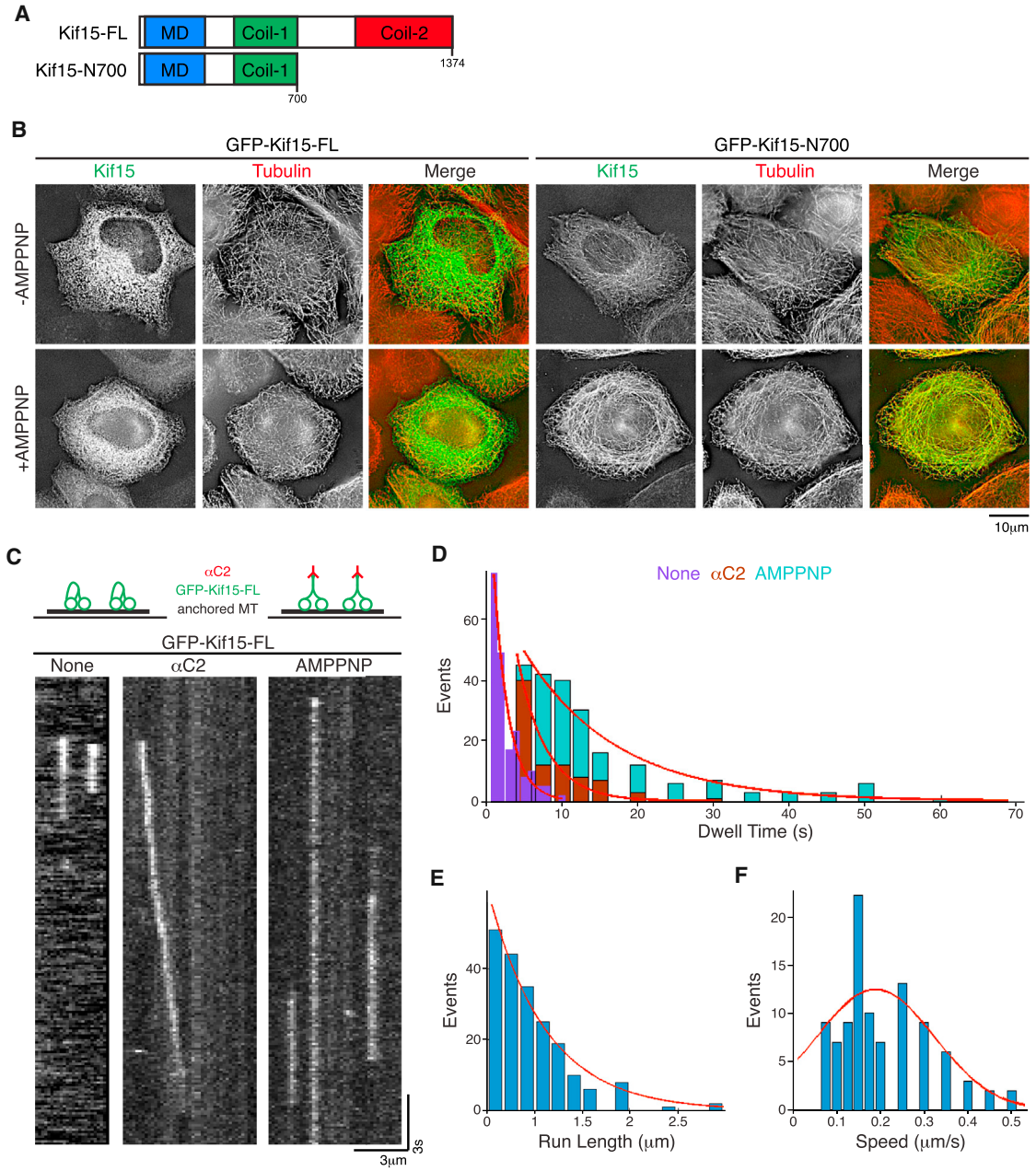

Figure 1. Kif15 Is Self-Repressed by Its C-Terminal Coil-2

(A) Schematic of Kif15 constructs. The motor domain (MD, blue), Coil-1 (green), and Coil-2 (red) regions are indicated. Numbers represent amino acid residues.

(B) Representative single focal planes of HeLa cells expressing GFP-Kif15-FL (left) or GFP-Kif15-N700 (right). Cells were left untreated (top) or infused with 1 mM AMPPNP (bottom). Kif15 (green) shows GFP fluorescence of indicated constructs. Tubulin (red) was detected by immunostaining. Individual channels are scaled identically. Scale bar, 10 μm. See also Figure S1A.

(C) Top, schematic of experimental conditions showing a coverslip (thin black line)-anchored MT (thick black line), GFP-Kif15-FL (green), and αC2 (red). Bottom, representative kymographs of single GFP-Kif15-FL molecules on MTs in the presence of ATP (left), ATP and αC2 (middle), or AMPPNP (right). See also Figures S1B, S1E, and S1F and Movie S2.

(D) Dwell-time distributions in seconds (s) from (C). Shown are GFP-Kif15-FL alone (purple), with αC2 (red), and with AMPPNP instead of ATP (teal). Mean dwell times were calculated from exponential fits (red) to the distributions.

(E) Run-length distribution of single GFP-Kif15-FL molecules complexed with αC2 from (C). Mean run length was calculated from an exponential fit (red) to the distribution.

(F) Speed distribution of single GFP-Kif15-FL molecules complexed with αC2 from (C). Mean speed was calculated from a fit of the distribution to a single Gaussian (red).

This relatively large SD may be attributable to the coexistence of active and repressed GFP-Kif15-FL molecules.

Although these data suggest that αC2 activates Kif15, we cannot rule out adverse effects from nonspecifically adsorbing GFP-Kif15-FL to flow cells. As a more rigorous test, we imaged single GFP-Kif15-FL molecules bound to MTs by time-lapse total internal reflection fluorescence (TIRF) microscopy. GFP-Kif15-FL appears dimeric, as the fluorescence of single

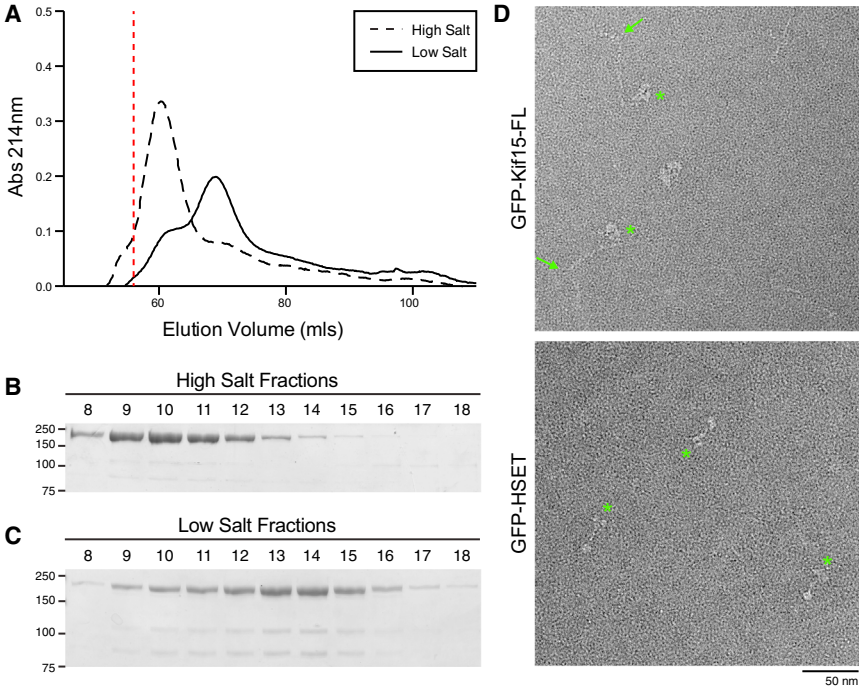

Figure 2. The Hydrodynamic Properties of Kif15 Are Salt Dependent

(A) Elution profiles of GFP-Kif15-FL from Superdex 200 16/60 sizing column runs in buffers of high salt (300 mM KCl, dashed line) and low salt (50 mM KCl, solid line). The void volume for the column is indicated by the red stippled line.

(B and C) SDS-PAGE of the indicated sizing column fractions run in buffers of high salt (B) or low salt (C) stained with Coomassie blue. Fractions 8–18 correspond to column eluates that span 57–79 ml. Molecular weight markers are indicated in kilodaltons.

(D) Representative fields of GFP-Kif15-FL (top) and GFP-HSET (bottom) particles as seen by negative-stain EM. Asterisks mark globular head regions and arrows indicate flexible regions. Scale bar, 50 nm.

molecules reduces to background in two steps (Figure S1E). Single GFP-Kif15-FL molecules bind MTs for 1.9 ± 0.3 s (n = 194) and are immotile (Figures 1C and 1D). AMPPNP increases this dwell time to 12.2 ± 2.3 s (n = 215, Figures 1C and 1D), which may be an underestimation due to photobleaching. Strikingly, GFP-Kif15-FL complexed with αC2 binds MTs for 4.0 ± 1.1 s (n = 83) and walks 0.6 ± 0.1 μm (n = 202) at 0.19 ± 0.07 μm s^{-1} (n = 101, Figures 1C–1F; Movie S2). Under our conditions, αC2 does not alter the fluorescence distribution or bleaching kinetics of single GFP-Kif15-FL molecules (Figure S1F). Taken together, these data show that Kif15 is self-repressed by its C-terminal Coil-2.

The Hydrodynamic Properties of Kif15 Are Salt Sensitive

Previous reports of kinesin self-repression highlight conformational folding in facilitating inhibitory intramolecular interactions [20, 21]. During sizing chromatography, GFP-Kif15-FL elutes near the void volume in buffers of high ionic strength (300 mM KCl), peaking at an elution volume of 60.3 ml of a sizing column optimized to resolve proteins <600 kDa (see Supplemental Experimental Procedures; Figures 2A and 2B). In buffers of low ionic strength (50 mM KCl), GFP-Kif15-FL shifts to an elution volume of 69 ml (Figures 2A and 2C), suggesting that intramolecular electrostatic interactions fold Kif15 into a compact conformation. Notably, the elution profile of GFP-Kif15-FL in low salt displays a "shoulder" left of the peak (Figure 2A). We suspect this represents a subpopulation of GFP-Kif15-FL in transitory conformations, because no impurities are evident by SDS-PAGE (Figure 2C). During sedimentation velocity analytical ultracentrifugation, ~50% of GFP-Kif15-FL sediments with a Svedberg value (S) of 4.0 (rmsd = 0.0041, Figure S2). Weighing 376.4 kDa, this suggests that GFP-Kif15-FL exists as a dimer in solution, in agreement with our single molecule data (Figure S1E). The high frictional ratio of 2.7 indicates that GFP-Kif15-FL is elongated, accounting for its anomalous migration during sizing chromatography in high salt.

Two short disordered regions are predicted to interrupt the otherwise coiled-coil stalk of Kif15 [3, 22, 23]. These regions could serve as "hinges" to enable conformational folding, so we next visualized GFP-Kif15-FL molecules by single-particle negative-stain electron microscopy (EM). Consistent with Kif15 existing as a dimer in its native state, single GFP-Kif15-FL molecules exhibit two globular domains likely corresponding to two GFP-fused motor heads (Figure 2D). A "kink" commonly interrupts the otherwise straight stalk of single GFP-Kif15-FL molecules (Figure 2D), which may correspond to a flexible hinge. To ensure that kinks are not artifacts introduced during sample preparation, we visualized the kinesin-14 HSET for comparison. The cherry-like appearance of single GFP-HSET molecules likely represents two C-terminal motor heads dimerized by a coiled-coil stalk extending to N-terminal GFP-tagged globular domains (Figure 2D; [24]). Importantly, single GFP-HSET molecules display no kinks (Figure 2D). Altogether, these data suggest that Kif15 toggles between open and closed conformations.

Kif15 Crosslinks and Slides MTs via a Second MT-Binding Site

To study the motile properties of constitutively active Kif15, we analyzed a C-terminally truncated construct (Kif15-N700, Figures 1A and S1B). Like GFP-Kif15-FL, recombinant Kif15-N700 dimerizes as assessed by sizing chromatography (data not shown). In conventional gliding assays, Kif15-N700 moves MTs at 0.184 ± 0.084 μm s^{-1} (n = 368, Figures 3A and 3B). Polarity marked MTs lead with their minus ends (Figure S3A), validating that Kif15 is plus-end-directed like its *Xenopus* ortholog Xklp2 [22].

Kif15-N700 robustly bundles MTs in solutions devoid of nucleotide (Figure 3C). In solutions containing ATP, Kif15-N700 crosslinks MTs with minimal overlap. This end-to-end MT "tiling" is detectable with two populations of monochromatically labeled MTs (Figure 3D). To visualize the remodeling of MT bundles into tiled arrays, we sandwiched Kif15-N700 between a coverslip-anchored red MT and a solution-derived green MT in flow cells. Kif15-N700 slides the cargo MT along the anchored MT upon ATP addition (Figure 3E; Movie S3), accounting for the nucleotide-dependent change in MT organization.

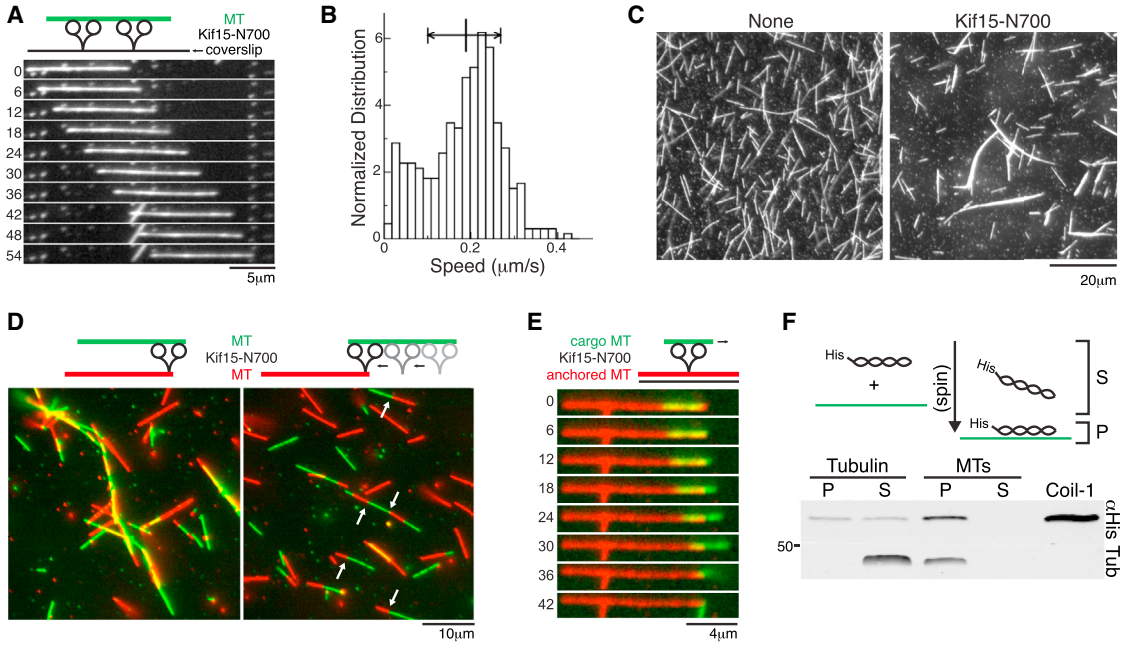

Figure 3. Kif15 Crosslinks and Slides Microtubules via a Second MT-Binding Site

(A) Top, schematic of experimental conditions showing coverslip (black line), GFP-Kif15-N700 (black), and fluorescent MT (green). Bottom, representative montage of a fluorescent MT in gliding assay with Kif15-N700. Numbers indicate time in seconds after initial frame. Scale bar, 5 μm. See also Figures S1B and S3A.

(B) Normalized distribution (each histogram count divided by the number of trajectories analyzed, n = 368) of MT speeds from (A). Vertical lines and horizontal arrows indicate average ±SD (0.184 ± 0.084 μm s^{-1}).

(C) Representative images of fluorescent MTs incubated in solution devoid of nucleotide in the absence (left) or presence (right) of Kif15-N700. Scale bar, 20 μm.

(D) Top, schematic of experimental conditions showing Kif15-N700 (black) and fluorescent MTs (red and green). Bottom, representative images of red and green fluorescent MTs incubated in solution with Kif15-N700 in the absence (left) or presence (right) of 1 mM ATP. Arrows indicate examples of MT "tiling." Scale bar, 10 μm.

(E) Top, schematic of experimental conditions showing a coverslip (black line)-anchored MT (red), Kif15-N700 (black), and a solution-derived cargo MT (green). Bottom, representative montage of red and green MTs in a two-MT sliding assay with Kif15-N700 in 750 μM ATP. Numbers indicate time in seconds after initial frame. Scale bar, 4 μm. See also Movie S3.

(F) Top, schematic of experimental conditions showing Coil-1 (black) and MTs (green). Bottom, blot of fractions from a MT copelleting assay with Kif15-Coil-1. Supernatant "S" and pellet "P" fractions are indicated. Kif15-Coil-1 was detected with α-His antibodies. Tubulin is also shown. Molecular weight markers are indicated in kDa. See also Figures S1B, S3B, and S3C.

The ability of Kif15-N700 to bundle MTs independently of ATP suggests the presence of a nonmotor MT-binding site. We therefore tested the MT-binding capabilities of Coil-1 (amino acids 365–700, Figures 1A and S1B). Recombinant Kif15-Coil-1 copellets with MTs (Figures 3F and S3B), revealing that Kif15 harbors a nonmotor MT-binding site. For comparison, recombinant Kif15-Coil-2 does not copellet with MTs (Figures S1B and S3C). Altogether, these data show that dimeric Kif15 crosslinks and slides MTs as a consequence two-MT-binding sites.

Kif15 Accumulates on MT Bundles

In the case of kinesin-1, cargo binding activates motility [20]. A second MT could similarly activate Kif15 by binding Coil-1. In this scenario, MT bundles would induce robust Kif15 activity by simultaneously providing substrate for Coil-1 and the motor heads. GFP-Kif15-FL does not detectably associate with individual MTs in solution (Figure 4A), aligning with our single molecule data. However, GFP-Kif15-FL accumulates on MT bundles induced by PRC1 (Figures 4A and S4A), a MAP that bundles midzone MTs [25]. Like PRC1, TPX2 bundles MTs. TPX2 is thought to be a loading factor for Kif15 [3–5], but both PRC1 and TPX2 fail to recruit Kif15 to individual coverslip-bound MTs (Figure S4B). Altogether, these data indicate that Kif15 has an inherent affinity for MT bundles in vitro.

Not only does GFP-Kif15-FL accumulate on PRC1-bundled MTs, but single molecules dwell for 9.0 ± 1.3 s (n = 91) and move 0.4 ± 0.1 μm (n = 209) at 0.14 ± 0.03 μm s^{-1} (n = 100, Figures 4B–4E; Movie S4). These motility parameters contrast those of GFP-Kif15-FL on single MTs and suggest that, like αC2, MT bundles activate Kif15.

In mitotic cells, Kif15 enriches on K-fibers [1]. To test whether Kif15 recognizes this spindle MT population for their bundled configuration, we induced nonkinetochore-MT bundling with FCPT, an Eg5 rigor drug [2, 26]. Consistent with our previously published data, small interfering RNA (siRNA) depletion of the outer kinetochore component Nuf2 abrogates Kif15 spindle localization (Figure 4F) by preventing K-fiber formation [1, 27]. Strikingly, FCPT treatment restores Kif15 spindle localization in Nuf2-depleted cells (Figure 4F), revealing that Kif15 can bind bundled nonkinetochore-MTs. FCPT does not dramatically alter the distribution of Kif15 on spindles in untreated cells or mock-depleted cells (Figures 4F and S4C). We propose that Kif15 normally targets K-fibers because of its inherent affinity for MT bundles.

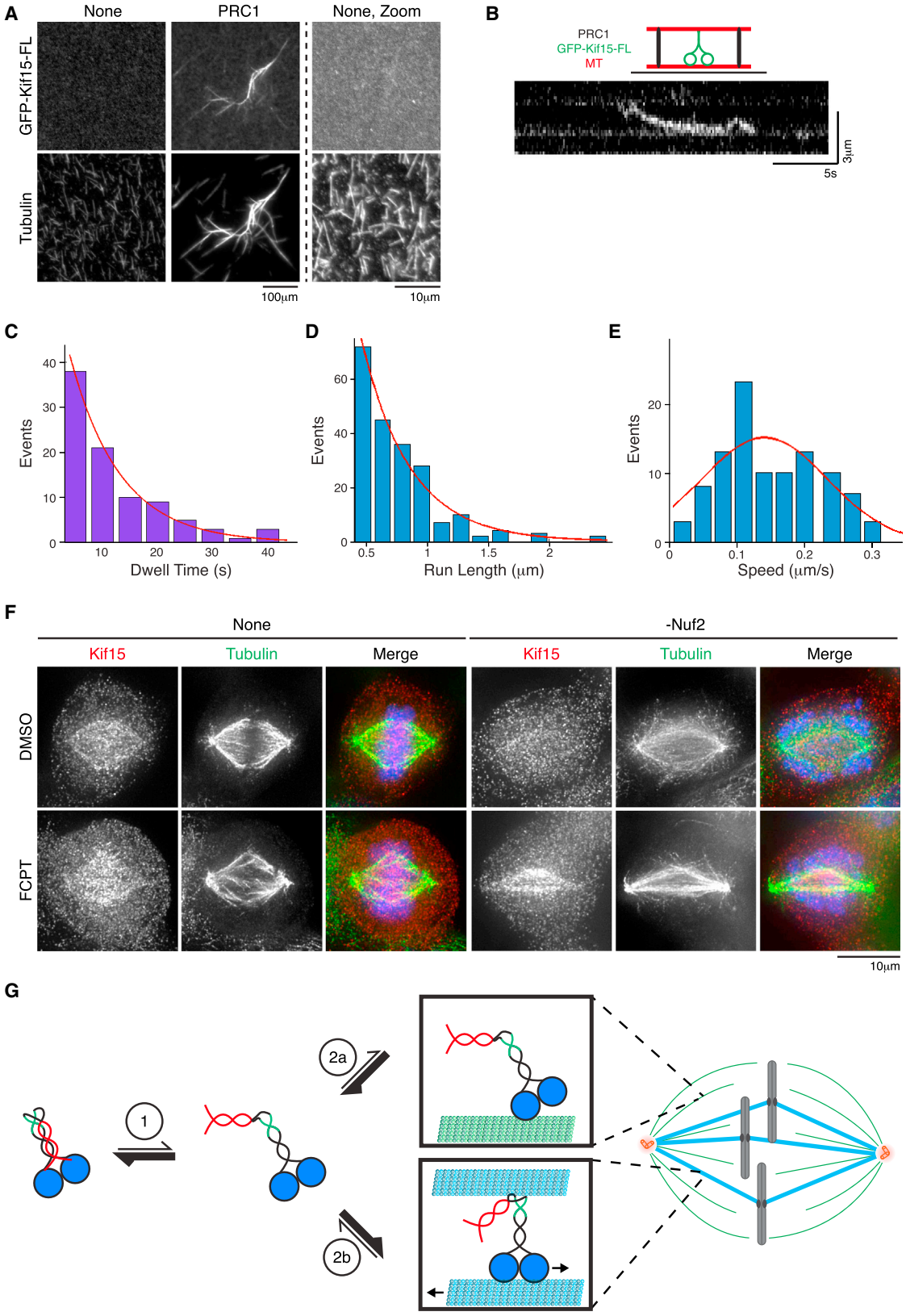

Figure 4. Kif15 Accumulates on MT Bundles

(A) Representative images of GFP-Kif15-FL on individual (left) or PRC1-bundled (right) fluorescent MTs in solution. Individual MTs are also shown at higher magnification. Individual channels were scaled identically. Scale bar, 100 (left) or 10 μm (right). See also Figures S4A and S4B.

(B) Top, schematic of experimental conditions showing coverslip (thin black line), GFP-Kif15-FL (green), fluorescent MTs (red), and PRC1 (black). Bottom, representative kymograph showing movement of GFP-Kif15-FL within PRC1-bundled MTs. See also Movie S4.

(legend continued on next page)

Discussion

Most kinesin-targeting mechanisms rely on motor-track affinity or extrinsic targeting factors. For example, kinesin-1 selectively binds MTs that are acetylated or GTP-tubulin rich [28]. On the other hand, the mitotic kinesin Xklp1 accumulates on antiparallel midzone MTs through transient interactions with PRC1 [24]. In contrast to these previously described mechanisms, our data suggest that Kif15 targets K-fibers because of its inherent affinity for MT bundles. This conclusion is supported by two key findings. First, Kif15 binds nonkinetochore-MTs only when they are bundled, as in Eg5-independent cells [1] and FCPT-treated HeLa cells (Figure 4F). Second, Kif15 selectively accumulates on MT bundles in vitro, such as those formed by PRC1 (Figure 4A) and TPX2 [29].

Although PRC1 has no known physiological interaction with Kif15, TPX2 has been proposed to recruit Kif15 to spindle MTs through a specific protein-protein interaction [3–5]. In support of this notion, TPX2 depletion abrogates Kif15 spindle localization [3, 4]. But like Nuf2 depletion, TPX2 depletion also prevents K-fiber formation [11, 30]. We therefore suspect that a loss of Kif15 spindle localization in TPX2-depleted cells is an indirect consequence of failed K-fiber formation. Similarly, we suspect that Kif15 associates with MTs in the presence of TPX2 in vitro simply because the MTs are bundled. Consistent with this idea, previous experiments implicating a direct TPX2-Kif15 interaction required the presence of MTs [5]. Additionally, we show that TPX2 is unsuccessful in recruiting Kif15 to individual MTs (Figure S4B). Our findings raise the possibility that Kif15 targets K-fibers via an intrinsic two-step mechanism (Figure 4G).

In our model, Kif15 autonomously targets K-fibers by (1) molecular unfolding and (2) two-MT binding. First, cytosolic Kif15 toggles between closed and open conformations, with a tendency for the closed conformation. Mediated by intramolecular electrostatic interactions, the closed conformation juxtaposes Coil-2 and the motor heads to sterically hinder MT binding. A nonmotor MT-binding site becomes exposed when Kif15 transiently unfolds, allowing Kif15 to engage MTs with its motor heads and/or Coil-1. If Kif15 engages a single MT with one binding site, it rapidly unbinds and collapses back to a closed conformation. Because most nonkinetochore-MTs are solitary and short lived, Kif15 does not appreciably concentrate on this spindle MT population at steady-state. On the other hand, if Kif15 simultaneously engages two MTs with both binding sites, it becomes locked in an open and active conformation. Because MTs within a K-fiber are bundled and long-lived, they are conducive to two-MT-binding and promote Kif15 activation.

An important direction for future work concerns the activity of Kif15 in MT bundles, a point underscored by the ability of Kif15 to differentially affect spindle assembly and length homeostasis as a function of the MT population to which it is bound [1]. Our findings demonstrate that dimeric Kif15 can combine its motor and nonmotor MT-binding sites to slide two MTs apart. Analogous to kinesin-14/Ncd and kinesin-8/Kip3 [31, 32], Kif15 might accomplish this by engaging one MT with its motor heads while holding a second MT with Coil-1. In this scenario, the strength of the Coil-1-MT interaction would dictate the consequence of Kif15 motility within a MT bundle. For example, diffusive Coil-1-MT interactions would allow Kif15 to move within a MT bundle, similar to Xklp1 [24]. On the other hand, strong Coil-1-MT interactions that exceed the Kif15 stall force would cause energy to be stored in the MT bundle as mechanical strain. We suspect these are key to understanding the mechanics of the Kif15-dependent "reverse jackknifing" spindle assembly mechanism that predominates in Eg5-independent cells [1].

Supplemental Information

Supplemental Information includes Supplemental Experimental Procedures, four figures, and four movies and can be found with this article online at http://dx.doi.org/10.1016/j.cub.2014.08.022.

Acknowledgments

We thank Aaron Groen and Tim Mitchison for FCPT and Radhika Subramanian and Tarun Kapoor for the PRC1 bacterial expression vector. Matt Tyska and the staff at the laboratories of M.J.L. and R.O. provided invaluable discussions and critical reading of the manuscript. This work was supported by VUMC Integrated Biological Systems Training in Oncology grant 5T32CA119925 to E.G.S.; American Heart Association grant 12PRE11750029 to E.G.S.; a fellowship from the Chambers Medical Foundation to D.K.D.; VUMC Molecular Biophysics training grant T32 GM08320 to S.E.C.; a Samsung Scholarship from the Samsung Foundation of Culture to Y.S.; and NIH grants R01 GM087677 to W.H. and M.J.L. and R01 GM086610 to R.O. M.J.L. was also supported by funds from the Singapore-Massachusetts Institute of Technology Alliance for Research and Technology. R.O. is a Scholar of the Leukemia and Lymphoma Society.

Received: June 5, 2014
Revised: July 28, 2014
Accepted: August 13, 2014
Published: September 25, 2014

References

1. Sturgill, E.G., and Ohi, R. (2013). Kinesin-12 differentially affects spindle assembly depending on its microtubule substrate. Curr. Biol. *23*, 1280–1290.
2. Vladimirou, E., Mchedlishvili, N., Gasic, I., Armond, J.W., Samora, C.P., Meraldi, P., and McAinsh, A.D. (2013). Nonautonomous movement of chromosomes in mitosis. Dev. Cell *27*, 60–71.
3. Tanenbaum, M.E., Macůrek, L., Janssen, A., Geers, E.F., Alvarez-Fernández, M., and Medema, R.H. (2009). Kif15 cooperates with eg5 to promote bipolar spindle assembly. Curr. Biol. *19*, 1703–1711.
4. Vanneste, D., Takagi, M., Imamoto, N., and Vernos, I. (2009). The role of Hklp2 in the stabilization and maintenance of spindle bipolarity. Curr. Biol. *19*, 1712–1717.

(C) Dwell-time distribution in seconds (s) of single GFP-Kif15-FL molecules within PRC1-bundled MTs from (B). Mean dwell time was calculated from an exponential fit (red) to the distribution.
(D) Run-length distribution of single GFP-Kif15-FL molecules within PRC1-bundled MTs from (B). Mean run length was calculated from an exponential fit (red) to the distribution.
(E) Speed distribution of single GFP-Kif15-FL molecules within PRC1-bundled MTs from (B). Mean speed of single GFP-Kif15-FL molecules was calculated from a fit of the distribution to a single Gaussian (red).
(F) Representative maximum Z-projections of Kif15 localization in HeLa cells treated with DMSO (top) or 200 μM FCPT (bottom) that have been untransfected (left) or siRNA-depleted of Nuf2 (right). Kif15 (red) and tubulin (green) were detected by immunostaining. DNA (blue) was counterstained with Hoechst 33342. Individual channels were scaled identically. Scale bar, 10 μm. See also Figure S4C.
(G) Model: Kif15 targets K-fibers via an intrinsic two-step mechanism. Motor heads (blue), Coil-1 (green), and Coil-2 (red) regions are indicated. See text for details.

5. Wittmann, T., Wilm, M., Karsenti, E., and Vernos, I. (2000). TPX2, A novel xenopus MAP involved in spindle pole organization. J. Cell Biol. *149*, 1405–1418.
6. Walczak, C.E., and Heald, R. (2008). Mechanisms of mitotic spindle assembly and function. Int. Rev. Cytol. *265*, 111–158.
7. Welburn, J.P. (2013). The molecular basis for kinesin functional specificity during mitosis. Cytoskeleton *70*, 476–493.
8. Kapitein, L.C., Peterman, E.J., Kwok, B.H., Kim, J.H., Kapoor, T.M., and Schmidt, C.F. (2005). The bipolar mitotic kinesin Eg5 moves on both microtubules that it crosslinks. Nature *435*, 114–118.
9. Ferenz, N.P., Gable, A., and Wadsworth, P. (2010). Mitotic functions of kinesin-5. Semin. Cell Dev. Biol. *21*, 255–259.
10. Raaijmakers, J.A., van Heesbeen, R.G., Meaders, J.L., Geers, E.F., Fernandez-Garcia, B., Medema, R.H., and Tanenbaum, M.E. (2012). Nuclear envelope-associated dynein drives prophase centrosome separation and enables Eg5-independent bipolar spindle formation. EMBO J. *31*, 4179–4190.
11. Bird, A.W., and Hyman, A.A. (2008). Building a spindle of the correct length in human cells requires the interaction between TPX2 and Aurora A. J. Cell Biol. *182*, 289–300.
12. Mack, G.J., and Compton, D.A. (2001). Analysis of mitotic microtubule-associated proteins using mass spectrometry identifies astrin, a spindle-associated protein. Proc. Natl. Acad. Sci. USA *98*, 14434–14439.
13. Mayr, M.I., Hümmer, S., Bormann, J., Grüner, T., Adio, S., Woehlke, G., and Mayer, T.U. (2007). The human kinesin Kif18A is a motile microtubule depolymerase essential for chromosome congression. Curr. Biol. *17*, 488–498.
14. Silljé, H.H., Nagel, S., Körner, R., and Nigg, E.A. (2006). HURP is a Ran-importin beta-regulated protein that stabilizes kinetochore microtubules in the vicinity of chromosomes. Curr. Biol. *16*, 731–742.
15. Wong, J., and Fang, G. (2006). HURP controls spindle dynamics to promote proper interkinetochore tension and efficient kinetochore capture. J. Cell Biol. *173*, 879–891.
16. Mayr, M.I., Storch, M., Howard, J., and Mayer, T.U. (2011). A non-motor microtubule binding site is essential for the high processivity and mitotic function of kinesin-8 Kif18A. PLoS ONE *6*, e27471.
17. Stumpff, J., Du, Y., English, C.A., Maliga, Z., Wagenbach, M., Asbury, C.L., Wordeman, L., and Ohi, R. (2011). A tethering mechanism controls the processivity and kinetochore-microtubule plus-end enrichment of the kinesin-8 Kif18A. Mol. Cell *43*, 764–775.
18. Cai, D., Hoppe, A.D., Swanson, J.A., and Verhey, K.J. (2007). Kinesin-1 structural organization and conformational changes revealed by FRET stoichiometry in live cells. J. Cell Biol. *176*, 51–63.
19. Hammond, J.W., Cai, D., Blasius, T.L., Li, Z., Jiang, Y., Jih, G.T., Meyhofer, E., and Verhey, K.J. (2009). Mammalian Kinesin-3 motors are dimeric in vivo and move by processive motility upon release of autoinhibition. PLoS Biol. *7*, e72.
20. Verhey, K.J., and Hammond, J.W. (2009). Traffic control: regulation of kinesin motors. Nat. Rev. Mol. Cell Biol. *10*, 765–777.
21. Hackney, D.D., Levitt, J.D., and Suhan, J. (1992). Kinesin undergoes a 9 S to 6 S conformational transition. J. Biol. Chem. *267*, 8696–8701.
22. Boleti, H., Karsenti, E., and Vernos, I. (1996). Xklp2, a novel Xenopus centrosomal kinesin-like protein required for centrosome separation during mitosis. Cell *84*, 49–59.
23. Klejnot, M., Falnikar, A., Ulaganathan, V., Cross, R.A., Baas, P.W., and Kozielski, F. (2014). The crystal structure and biochemical characterization of Kif15: a bifunctional molecular motor involved in bipolar spindle formation and neuronal development. Acta Crystallogr. D Biol. Crystallogr. *70*, 123–133.
24. Bieling, P., Telley, I.A., and Surrey, T. (2010). A minimal midzone protein module controls formation and length of antiparallel microtubule overlaps. Cell *142*, 420–432.
25. Subramanian, R., and Kapoor, T.M. (2012). Building complexity: insights into self-organized assembly of microtubule-based architectures. Dev. Cell *23*, 874–885.
26. Groen, A.C., Needleman, D., Brangwynne, C., Gradinaru, C., Fowler, B., Mazitschek, R., and Mitchison, T.J. (2008). A novel small-molecule inhibitor reveals a possible role of kinesin-5 in anastral spindle-pole assembly. J. Cell Sci. *121*, 2293–2300.
27. DeLuca, J.G., Moree, B., Hickey, J.M., Kilmartin, J.V., and Salmon, E.D. (2002). hNuf2 inhibition blocks stable kinetochore-microtubule attachment and induces mitotic cell death in HeLa cells. J. Cell Biol. *159*, 549–555.
28. Nakata, T., Niwa, S., Okada, Y., Perez, F., and Hirokawa, N. (2011). Preferential binding of a kinesin-1 motor to GTP-tubulin-rich microtubules underlies polarized vesicle transport. J. Cell Biol. *194*, 245–255.
29. Drechsler, H., McHugh, T., Singleton, M.R., Carter, N.J., and McAinsh, A.D. (2014). The Kinesin-12 Kif15 is a processive track-switching tetramer. eLife *3*, e01724.
30. Tulu, U.S., Fagerstrom, C., Ferenz, N.P., and Wadsworth, P. (2006). Molecular requirements for kinetochore-associated microtubule formation in mammalian cells. Curr. Biol. *16*, 536–541.
31. Braun, M., Drummond, D.R., Cross, R.A., and McAinsh, A.D. (2009). The kinesin-14 Klp2 organizes microtubules into parallel bundles by an ATP-dependent sorting mechanism. Nat. Cell Biol. *11*, 724–730.
32. Su, X., Arellano-Santoyo, H., Portran, D., Gaillard, J., Vantard, M., Thery, M., and Pellman, D. (2013). Microtubule-sliding activity of a kinesin-8 promotes spindle assembly and spindle-length control. Nat. Cell Biol. *15*, 948–957.